Mutational Specificity of γ-Radiation-Induced Guanine−Thymine and Thymine−Guanine Intrastrand Cross-Links in Mammalian Cells and Translesion Synthesis Past the Guanine −Thymine Lesi...

ARTICLE *in* BIOCHEMISTRY · JULY 2008

Impact Factor: 3.02 · DOI: 10.1021/bi800529f · Source: PubMed

3 AUTHORS, INCLUDING:

Ashis Basu
University of Connecticut
109 PUBLICATIONS **3,317** CITATIONS

SEE PROFILE

Mutational Specificity of γ-Radiation-Induced Guanine−Thymine and Thymine−Guanine Intrastrand Cross-Links in Mammalian Cells and Translesion Synthesis Past the Guanine−Thymine Lesion by Human DNA Polymerase η†

Laureen C. Colis, Paromita Raychaudhury, and Ashis K. Basu*

Department of Chemistry, University of Connecticut, Storrs, Connecticut 06269

Received March 27, 2008; Revised Manuscript Received May 21, 2008

ABSTRACT: Comparative mutagenesis of γ- or X-ray-induced tandem DNA lesions G[8,5-Me]T and T[5-Me,8]G intrastrand cross-links was investigated in simian (COS-7) and human embryonic (293T) kidney cells. For G[8,5-Me]T in 293T cells, 5.8% of progeny contained targeted base substitutions, whereas 10.0% showed semitargeted single-base substitutions. Of the targeted mutations, the G → T mutation occurred with the highest frequency. The semitargeted mutations were detected up to two bases 5′ and three bases 3′ to the cross-link. The most prevalent semitargeted mutation was a C → T transition immediately 5′ to the G[8,5-Me]T cross-link. Frameshifts (4.6%) (mostly small deletions) and multiple-base substitutions (2.7%) also were detected. For the T[5-Me,8]G cross-link, a similar pattern of mutations was noted, but the mutational frequency was significantly higher than that of G[8,5-Me]T. Both targeted and semitargeted mutations occurred with a frequency of ∼16%, and both included a dominant G → T transversion. As in 293T cells, more than twice as many targeted mutations in COS cells occurred in T[5-Me,8]G (11.4%) as in G[8,5-Me]T (4.7%). Also, the level of semitargeted single-base substitutions 5′ to the lesion was increased and 3′ to the lesion decreased in T[5-Me,8]G relative to G[8,5-Me]T in COS cells. It appeared that the majority of the base substitutions at or near the cross-links resulted from incorporation of dAMP opposite the template base, in agreement with the so-called "A-rule". To determine if human polymerase η (hpol η) might be involved in the mutagenic bypass, an in vitro bypass study of G[8,5-Me]T in the same sequence was carried out, which showed that hpol η can bypass the cross-link incorporating the correct dNMP opposite each cross-linked base. For G[8,5-Me]T, nucleotide incorporation by hpol η was significantly different from that by yeast pol η in that the latter was more error-prone opposite the cross-linked Gua. The incorporation of the correct nucleotide, dAMP, by hpol η opposite cross-linked T was 3−5-fold more efficient than that of a wrong nucleotide, whereas incorporation of dCMP opposite the cross-linked G was 10-fold more efficient than that with dTMP. Therefore, the nucleotide incorporation pattern by hpol η was not consistent with the observed cellular mutations. Nevertheless, at and near the lesion, hpol η was more error-prone compared to a control template. The in vitro data suggest that translesion synthesis by another Y-family DNA polymerase and/or flawed participation of an accessory protein is a more likely scenario in the mutagenesis of these lesions in mammalian cells. However, hpol η may play a role in correct bypass of the cross-links.

DNA damage by reactive oxygen species (ROS)[1] has been extensively studied for the past two decades (*1*). Types of ROS-induced DNA damage include single-base damage, strand breaks, and inter- and intrastrand DNA−DNA and DNA−protein cross-links (see ref *2* for a review). However, compared to single-base types of damage, which were thoroughly studied, complex lesions such as tandem DNA damage received relatively little attention (*3*). In a series of investigations in the late 1990s, Box and co-workers showed that double-base DNA lesions are formed at a substantial frequency by ionizing radiation and by metal-catalyzed H_2O_2 reactions (*4*–*7*). In the presence of oxygen, a major type of radiation-induced damage involves oxidation of a Gua to 8-oxoguanine and degradation of an adjacent pyrimidine base to a formamido remnant (*4*). Under anoxic conditions, the predominant lesion is a cross-linked species in which C8 of Gua is linked to the 5-methyl group of an adjacent Thy, but the G[8,5-Me]T cross-link is formed at a much higher rate than the T[5-Me,8]G cross-link (Figure 1) (*4*–*7*). Additional thymine−purine cross-links have been isolated from γ-irradiated DNA in oxygen-free aqueous solution (*8*). Wang and co-workers identified structurally similar guanine−cytosine and guanine−5-methylcytosine cross-links in DNA exposed

† This work was supported by the National Institute of Environmental Health Sciences, National Institutes of Health (Grant ES013324).

* To whom correspondence should be addressed: Department of Chemistry, University of Connecticut, Storrs, CT 06269. Telephone: (860) 486-3965. Fax: (860) 486-2981. E-mail: ashis.basu@uconn.edu.

[1] Abbreviations: G[8,5-Me]T or G^T, guanine−thymine intrastrand cross-link in which C8 of guanine is covalently bonded to the methyl carbon of the 3′-thymine; T[5-Me,8]G or T^G, thymine−guanine intrastrand cross-link in which C8 of guanine is covalently bonded to the methyl carbon of the 5′-thymine; Gua, guanine; Thy, thymine; Cyt, cytosine; MF, mutation frequency; ROS, reactive oxygen species; TLS, translesion synthesis; NER, nucleotide excision repair; hpol η, human DNA polymerase η.

10.1021/bi800529f CCC: $40.75
Published on Web 07/11/2008

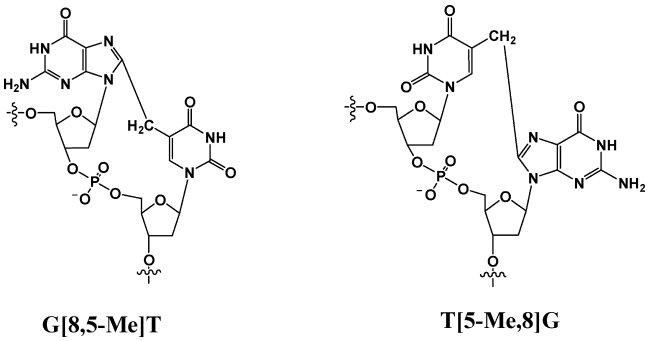

G[8,5-Me]T **T[5-Me,8]G**

FIGURE 1: Chemical structures of the two intrastrand cross-links.

to γ- or X-rays (*9–11*). Carter and Greenberg (*12*) showed that a pyrimidine nucleobase radical generates tandem lesions as the major modification, which could be as frequent as 65%. Recent investigations established that the G[8,5-Me]T cross-link is formed in a dose-dependent manner in human cells when exposed to γ-rays (*13*) and that the G[8,5]C cross-link is formed at a slightly lower level (*14*).

These intrastrand cross-links destabilize the DNA double helix (*15*), and it is not surprising that UvrABC nuclease, the nucleotide excision repair (NER) system in *Escherichia coli*, can excise G[8,5-Me]T in vitro (*16, 17*). Using purified DNA polymerases, it was shown that G[8,5-Me]T and G[8,5]C strongly block DNA replication in vitro (*13, 18*). For the G[8,5-Me]T cross-link, primer extension was terminated after incorporation of dAMP opposite the 3′-T by exo-free Klenow fragment and pol IV (dinB) of *E. coli*, whereas Taq polymerase was completely blocked at the nucleotide preceding the cross-link (*18*). However, yeast polymerase η, a member of the Y-family DNA polymerase, can bypass both G[8,5-Me]T and G[8,5]C cross-links, albeit with reduced efficiency relative to a control (*13, 17*). For these two lesions, the significantly reduced fidelity of nucleotide incorporation was observed at the 5′-Gua. The incorporation of dAMP and dGMP was favored by yeast pol η over that of the correct nucleotide, dCMP (*13, 17*). A recent study demonstrated that the G[8,5]C cross-link is mutagenic in *E. coli* (*14*). It induced ~10% mutations, which included mostly G → T transversions and a lower level of G → C substitutions. The mutations were almost completely abolished in the pol V-deficient strain, suggesting that this SOS polymerase is likely responsible for the error-prone translesion synthesis. However, the biological effect of these cross-links has not been investigated in mammalian cells. Also, cellular studies on any other purine−pyrimidine (or pyrimidine−purine) cross-links such as G[8,5-Me]T have not yet been reported.

In this work, we have compared translesion synthesis of G[8,5-Me]T with T[5-Me,8]G cross-links in simian and human embryonic kidney cells. We report here that both of these cross-links are strongly mutagenic in the two cell lines and that the two lesions exhibit an interesting pattern of mutations, including a high frequency of semitargeted or locally targeted mutations. To determine if pol η might play a role in the mutagenicity exhibited by these lesions in mammalian cells, we have also explored in vitro bypass of G[8,5-Me]T by purified human DNA polymerase η (hpol η).

MATERIALS AND METHODS

Materials. [γ-^{32}P]ATP was from Du Pont New England Nuclear (Boston, MA). *Eco*RV restriction endonuclease, T4 DNA ligase, T4 polynucleotide kinase, uracil DNA glycosylase, and exonuclease III were obtained from New England Bioloabs (Beverly, MA). *E. coli* DH10B was purchased from Invitrogen Corp. (Carlsbad, CA). Human and yeast DNA polymerase η were purchased from Enzymax (Lexington, KY). The simian kidney (COS-7) cell line available in our laboratory was originally obtained from P. Glazer (Yale University, New Haven, CT), and the pMS2 phagemid was a gift of M. Moriya (State University of New York, Stony Brook, NY). Human embryonic kidney cell line 293T/17 was purchased from American type Culture Collection (ATCC).

Methods. (i) Synthesis and Characterization of Oligonucleotides. The lesions containing oligonucleotides 5′-GTGCG^TGTTTGT-3′ and 5′-GTGCGT^GTTTGT-3′ have been synthesized and characterized as described previously (*16*). Unmodified oligonucleotides were analyzed by MALDI-TOF MS analysis, which gave a molecular ion with a mass within 0.005% of the theoretical mass, whereas adducted oligonucleotides were analyzed by ESI-MS in addition to digestion followed by HPLC analysis.

(ii) Construction of 26-mer Containing a G[8,5-Me]T Cross-Link. The modified 12-mer and a control 12-mer (~5 nmol) were ligated to a 5′-phosphorylated 14-mer, 5′-ATCGCTTGCAGGGG-3′ (~7.5 nmol), in the presence of an 18-mer complementary oligonucleotide, 5′-GCAAGC-GATACAAACACG-3′ (~7.5 nmol), as described previously (*19*). The oligonucleotides were separated by electrophoresis on a 16% polyacrylamide−8 M urea gel. The ligated product bands were visualized by UV shadowing and excised. The 26-mers were desalted on a Sephadex G-25 (Sigma) column and stored at −20 °C until further use.

(iii) Construction and Characterization of pMS2 Vectors Containing a Single G[8,5-Me]T or T[5-Me,8]G Cross-Link. The single-stranded pMS2 shuttle vector, which contains its only *Eco*RV site in a hairpin region, was prepared as described previously (*20*). The pMS2 DNA (58 pmol, 100 μg) was digested with a large excess of *Eco*RV (300 pmol, 4.84 μg) for 1 h at 37 °C followed by room temperature overnight. A 58-mer scaffold oligonucleotide was annealed overnight at 9 °C to form the gapped DNA. The control and lesion-containing oligonucleotides were phosphorylated with T4 polynucleotide kinase, hybridized to the gapped pMS2 DNA, and ligated overnight at 16 °C. Unligated oligonucleotides were removed by being passed through a Centricon-100, and the DNA was precipitated with ethanol. The scaffold oligonucleotide was digested by being treated with uracil DNA glycosylase and exonuclease III; the proteins were extracted with phenol and chloroform, and the DNA was precipitated with ethanol. The final construct was dissolved in 1 mM Tris-HCl and 0.1 mM EDTA (pH 8), and a portion was subjected to electrophoresis on a 1% agarose gel to assess the amount of circular DNA.

(iv) Replication and Analysis in Simian Kidney Cells. COS-7 cells were grown in Dulbecco's modified Eagle's medium supplemented with 10% fetal bovine serum. The cells were seeded at a density of 5×10^5 cells per 60 mm plate. Following overnight incubation, the cells were transfected with 50 ng of ssDNA by either electroporation or using 6

Scheme 1: General Protocol for Making the pMS2 Construct Followed by Replication and Analysis

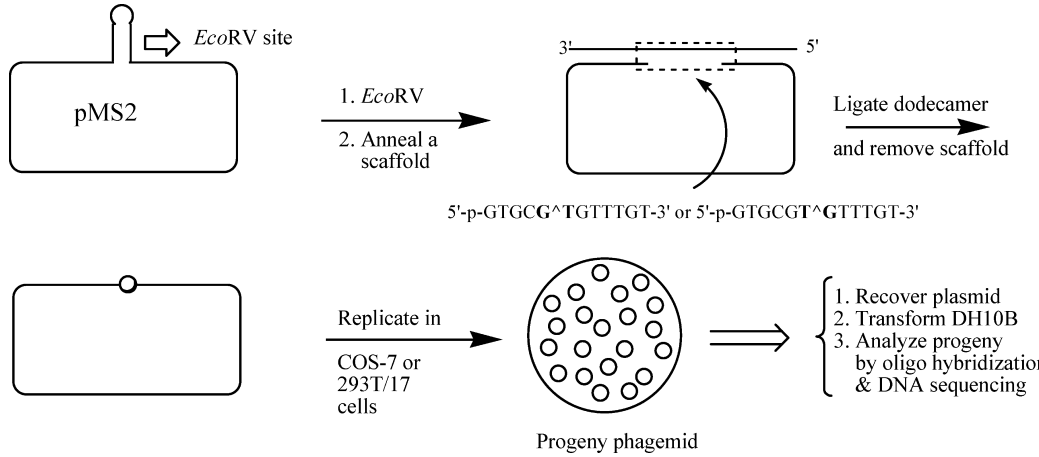

μL of Lipofectamine cationic lipid reagent (Invitrogen). The culture was incubated for 2 days, and the progeny plasmid was recovered by the method of Hirt (*21*). It was then used to transform *E. coli* DH10B, and transformants were analyzed by oligonucleotide hybridization (*22*). Oligonucleotide probes containing the complementary 16-mer sequence were used to analyze progeny phagemids. The 14-mer left and 15-mer right probes were used to select phagemids containing the correct insert, and transformants that did not hybridize with both the left and right probes were omitted. Any transformant that hybridized with the left and right probes but failed to hybridize with the 16-mer wild-type probe was subjected to DNA sequence analysis.

(v) Replication and Analysis in Human Embryonic Kidney (293T/17) Cells. The 293T/17 cell line is a derivative of the 293T cell line (293tsA1609neo). It is a highly transfectable derivative of the 293 cell line into which the temperature-sensitive gene for simian virus 40 (SV40) T antigen was inserted. These cells constitutively express the SV40 large T antigen.

The 293T/17 cells were maintained in Dulbecco's modified Eagle's medium supplemented with 4 mM L-glutamine and adjusted to contain 1.5 g/L sodium bicarbonate, 4.5 g/L glucose, and 10% fetal bovine serum. The cells were grown to ~90% confluency and transfected with 50 ng of each construct using 6 μL of Lipofectamine cationic lipid reagent (Invitrogen). Following transfection with modified or unmodified pMS2, the cells were allowed to grow at 37 °C in 5% CO_2 for 2 days, and then the plasmid DNA was collected and purified by the method of Hirt (*21*). Subsequent transformation in *E. coli* DH10B and analysis were performed in a manner similar to that for the plasmid from COS cells.

(vi) In Vitro Nucleotide Incorporation and Chain Extension. The 26-mer G[8,5-Me]T template, 5′-GTGCG^TGTTTGTATCGCTTGCAGGGG-3′, was constructed by ligating a 14-mer to the G[8,5-Me]T cross-linked 12-mer, followed by purification. The primed template was obtained by annealing a 5-fold molar excess of the modified or control 26-mer template (~20 ng) to a complementary 5′-^{32}P-labeled primer. For full-length extensions, the ^{32}P-labeled primer (14-, 15-, 16-, or 17-mer) template complex was incubated with 50 nM hpol η and a mixture of four dNTPs (25 mM each) in 25 mM Tris-HCl buffer (pH 7.5), 5 mM $MgCl_2$, and 5 mM dithiothreitol at 37 °C for various amounts of time. The reactions were terminated by adding an equal volume of 95% (v/v) formamide, 20 mM EDTA, 0.02% (w/v) xylene cyanol, and 0.02% (w/v) bromophenol blue and heating the mixture at 90 °C for 2 min, and the products were resolved on a 20% polyacrylamide gel containing 8 M urea.

(vii) Steady-State Kinetic Measurements. To identify the nucleotide preferentially incorporated opposite the G[8,5-Me]T cross-link, the steady-state kinetic analyses were performed by the method of Goodman and co-workers (*23–25*). Prior to kinetic studies, experiments were conducted to determine enzyme concentrations, dNTP concentrations, and times for which product accumulation was linear as a function of time. The dNTP concentration and time of incubation were optimized to ensure that the extent of primer extension was <20%. Primer extension of the primer−template complex (10 nM) under standing start conditions was carried out with a hpol η (6.4 nM for control and 16 nM for G[8,5-Me]T) with individual dNTPs in 25 mM Tris-HCl buffer (pH 7.5), 5 mM $MgCl_2$, and 5 mM dithiothreitol at 37 °C for various amounts of time. The reactions were terminated and the products resolved as described above. The DNA bands were visualized and quantitated using a Phosphorimager. The apparent K_m and V_{max} values were extrapolated from a Hanes−Woolf plot of the kinetic data (*23*). The efficiency of nucleotide incorporation was determined by V_{max}/K_m values. The fidelity of nucleotide incorporation was determined by the frequency of misincorporation (F_{inc}), according to the equation $F_{inc} = (V_{max}/K_m)$[wrong pair]/(V_{max}/K_m)[right pair].

RESULTS

Construction and Characterization of the sspMS2 Vector Containing the G[8,5-Me]T or T[5-Me,8]G Cross-Link and Its Replication in Mammalian Cells. To investigate translesion synthesis in SV-40-transformed simian kidney cell line COS-7 and human embryonic kidney cell line 293T, we employed a site-specifically modified single-stranded vector, pMS2, which confers neomycin and ampicillin resistance (*20, 26*). Biological effects of many types of DNA damage have been studied by using this vector developed by Moriya (*20*), and the strategy for employing this plasmid is shown in Scheme 1. Briefly, the double-stranded hairpin region of pMS2 ssDNA was digested with *Eco*RV, and the linear DNA

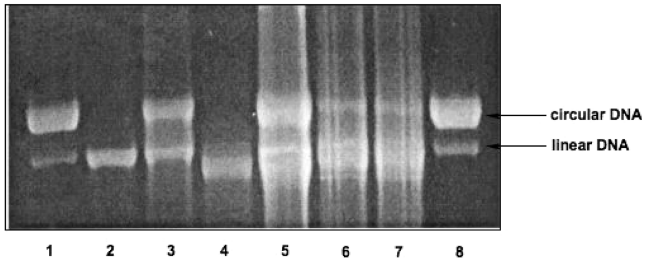

FIGURE 2: Agarose gel analysis of the pMS2 constructs. Lanes 1 and 8 show pMS2 DNA, whereas lane 2 shows the same after digestion with *Eco*RV. Lanes 3 and 4 represent the construct before and after the removal of the scaffold, respectively, of a mock ligation mixture, which did not contain a dodecamer. Lanes 5−7 show pMS2 constructs containing control, T[5-Me,8]G, and G[8,5-Me]T dodecamer, respectively, after enzymatic removal of the scaffold 58-mer.

was hybridized with a scaffold 58-mer to yield a gapped DNA. The oligonucleotides containing G[8,5-Me]T, T[5-Me,8]G, and a control were ligated to this gap. The control and lesion-containing constructs were treated with uracil DNA glycosylase and exonuclease III to remove the scaffold. A portion of each of these vectors was run on a 1% agarose gel. As shown in Figure 2, lanes 1 and 2 show migration characteristics of pMS2 DNA before and after digestion with *Eco*RV. Lanes 5−7 show ligation of control, T[5-Me,8]G-containing, and G[8,5-Me]T-containing 12-mer, respectively, to pMS2 followed by enzymatic removal of the scaffold. Lanes 3 and 4 show the construct before and after removal of the scaffold, respectively, of a "mock" ligation mixture, in which no oligonucleotide was added. It is evident from lanes 3 and 4 that end-to-end ligation of the scaffolded linear DNA in the absence of the appropriate insert was negligible. Estimation of the relative intensity of the circular and linear DNA indicated 30−50% ligation of the 12-mers occurred on both sides and that ligation of the control was nearly twice as efficient as that of the lesion-containing oligonucleotides.

The vectors containing the cross-links were used to transfect COS-7 or 293T cells. Progeny phagemids were recovered and used to transform *E. coli* DH10B. Transformants were analyzed by oligonucleotide hybridization followed by DNA sequencing (*22*), to confirm the number of progeny derived that contained the oligonucleotide insert and the mutational outcome of the lesions.

Mutational Specificity of G[8,5-Me]T and T[5-Me,8]G Cross-Links. As shown in Table 1 and Figure 3, both G[8,5-Me]T and T[5-Me,8]G cross-links exhibited significant mutagenicity in both 293T and COS-7 cells, although 62−77% progeny were derived from error-free bypass. In each case, mutations were analyzed for two independently constructed vectors, and though mutagenesis data were consistent in these transfections (Table 1), they were combined for the ease of analysis. A striking feature of the mutational spectra of the cross-links is that both lesions induced a large number of mutations at bases near the lesion, which we describe as semitargeted mutations (Table 1 and Figure 3) (see also Table S1 of the Supporting Information). It is important to point out that for the control construct, no mutations were detected within the 12-mer sequence in approximately 300 progeny that were analyzed (data not shown). For G[8,5-Me]T in 293T cells, 5.8% of progeny contained targeted base substitutions, whereas 10.0% exhibited semitargeted single-base substitutions. Of the targeted mutations, the G → T mutation occurred with the highest frequency (4.6%). The semitargeted mutations were detected up to two bases 5′ and three bases 3′ to the cross-link (Figure 4). However, the most prevalent semitargeted mutations involved a C → T transition (4.6%) immediately 5′ to the G[8,5-Me]T cross-link (Figure 4). In addition, multiple-base substitutions, predominantly two base substitutions, occurred at a frequency of 2.7% (Table S1 of the Supporting Information). Frameshifts, which included mostly deletions of one to four bases, were detected in 4.6% of progeny (Table 1 and Figure 3) (see also Table S1 of the Supporting Information). For the T[5-Me,8]G cross-link, although the mutational frequency increased, a similar pattern of mutations was noted. Targeted mutations occurred with a frequency of 16.3%, with the G → T mutation being the dominant event (14.3%) (Table 1 and Figure 5). The semitargeted single-base substitutions were detected up to three bases 5′ and three bases 3′ to the cross-link. They occurred at a frequency of 15.8%, of which the G immediately 5′ to the cross-link gave the highest frequency of G → T substitutions (Figure 5). Multiple-base substitutions and frameshifts were detected at frequencies of 2.0 and 3.6%, respectively (Table 1 and Figure 3) (see also Table S1 of the Supporting Information).

As in the case of 293T cells, more than twice as many targeted mutations in COS cells occurred in T[5-Me,8]G (11.4%) relative to G[8,5-Me]T (4.7%) (Table 1 and Figure 3). Also, as in 293T cells, the number of semitargeted base substitutions 5′ to the lesion was increased and 3′ to the lesion decreased in T[5-Me,8]G relative to G[8,5-Me]T in COS cells (Table 1). As shown in Figures 4 and 5, like the 293T cells, qualitatively a similar pattern of mutagenesis emerged from the progeny from COS-7 cells. Even so, certain differences were evident. For example, for the G[8,5-Me]T cross-link, the number of G → T and G → C mutations immediately 3′ and base substitutions at the third base 3′ (a T) increased significantly in COS cells relative to 293T cells (Figure 4). In a similar vein, for the T[5-Me,8]G cross-link, the number of G → T substitutions at the 5′ neighboring base decreased, whereas the number of C → T transitions at the second base 5′ to the lesion increased in COS cells relative to 293T cells (Figure 5). It is interesting that for the G[8,5-Me]T cross-link, the T three bases 3′ to the lesion, located in the middle of three consecutive thymines, exhibited much higher MF particularly in COS cells compared to the

Table 1: Mutational Frequencies of G[8,5-Me]T and T[5-Me,8]G Cross-Links in 293T and COS-7 Cells

	G^T in 293T	T^G in 293T	G^T in COS-7	T^G in COS-7
targeted at G	4.6 ± 0.6	14.3 ± 3.6	3.7 ± 1.9	10.6 ± 5.4
targeted at T	1.2 ± 0.2	2.0 ± 0.9	1.0 ± 0.6	0.7 ± 0.02
semitargeted 5′ to the cross-link	5.4 ± 1.4	11.7 ± 2.1	4.4 ± 2.8	7.0 ± 0.7
semitargeted 3′ to the cross-link	4.6 ± 0.7	4.1 ± 1.9	9.1 ± 2.2	2.6 ± 1.5
frameshift	4.6 ± 0.7	3.6 ± 1.7	4.4 ± 0.9	2.9 ± 1.1
multiple substitutions	2.7 ± 0.06	2.0 ± 0.5	1.3 ± 0.8	0.7 ± 0.02

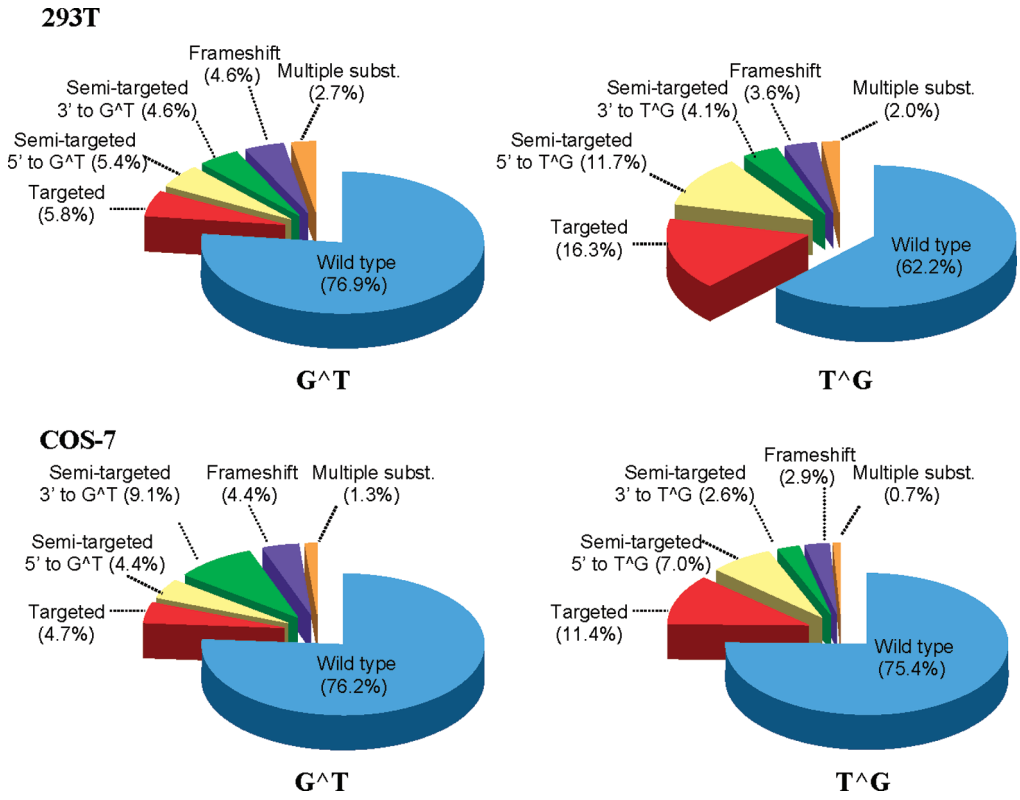

FIGURE 3: Analyses of the progeny derived from replicating the lesion-containing pMS2 constructs in COS-7 and 293T cells.

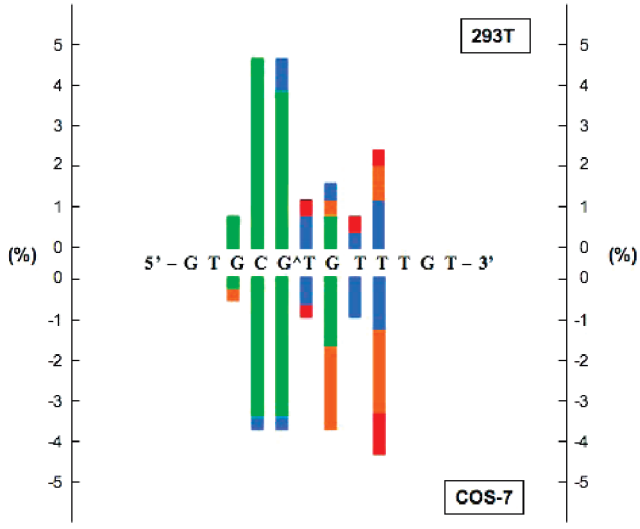

FIGURE 4: Types and frequencies of single-base substitutions induced by G[8,5-Me]T detected in 293T (top) and COS-7 (bottom) cells. The colors used in the bar graph represent T (green), A (blue), G (red), and C (orange).

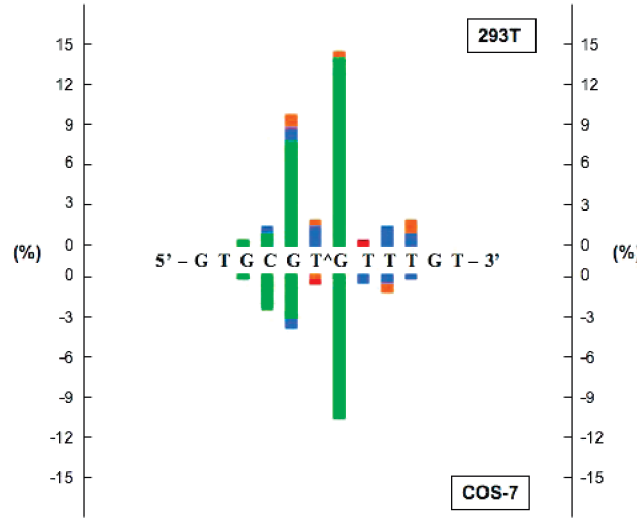

FIGURE 5: Types and frequencies of single-base substitutions induced by T[5-Me,8]G detected in 293T (top) and COS-7 (bottom) cells. The colors represent what they do in Figure 4.

cross-linked T (Figure 4). However, for the T[5-Me,8]G lesion, this T exhibited only modest MF (Figure 5). The complex nature of base substitutions induced by these two intrastrand cross-links was evident from the bar graphs showing the single-base substitutions in Figures 4 and 5.

The mutagenesis data of these two lesions in two different mammalian cell lines indicate a high error rate not only opposite the lesion but also in the local region, which suggests involvement of an error-prone Y-family DNA polymerase in TLS. What we also found remarkable is that there were many base substitutions that arose from incorporation of dAMP opposite either the cross-link or the bases near it. At or near the cross-links, four of the eight bases are thymines. The majority of the base substitutions at the four other bases (two cytosines and two guanines) were C → T and G → T substitutions, which appear to follow the A-rule (*27, 28*) of preferential incorporation of A opposite noninstructional lesions. The A-rule is consistent not only with the type of mutations observed but also with why the number of mutations at the cross-linked thymine was low.

In Vitro Bypass by hpol η. Previous studies have shown the G[8,5-Me]T cross-link to strongly block DNA replication by prokaryotic DNA polymerase (*18*), whereas yeast pol η can bypass both G[8,5]C and G[8,5-Me]T cross-links, albeit much more slowly than a control (*13, 15*). Since G[8,5-Me]T is mutagenic in human cells, we decided to investigate if hpol η can bypass this lesion and, in the event of translesion

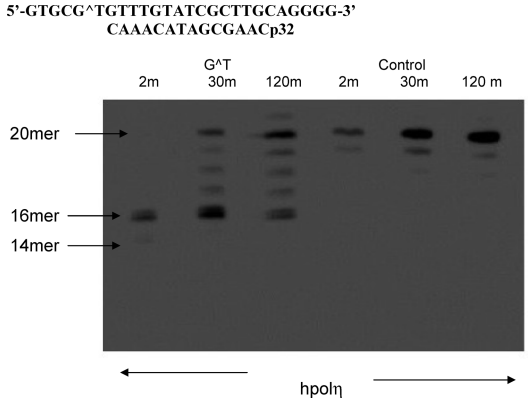

FIGURE 6: Extension of a 14-mer primer at 37 °C by hpol η (50 nM) in the presence of all four dNTPs (25 mM each).

synthesis, the specificity of nucleotide incorporation. For the in vitro experiment, a 26-mer template, 5′-GTGCG^TG-TTTGTATCGCTTGCAGGGG-3′, was constructed, which contained the G[8,5-Me]T cross-link (G^T) at the fifth and sixth bases from the 5′ end. As shown in Figure 6, in the presence of all four dNTPs, extension of a 14-mer primer on the control rapidly generated a full-length extension product (a 20-mer) in 2 min with 50 nM hpol η, whereas the extension of the primer stalled after addition of a base opposite the cross-linked T and G. Longer incubation allowed further extension, including a full-length product, but even after 2 h, significant 16−19-mer extension products remained.

Since hpol η can bypass the G[8,5-Me]T cross-link, we determined steady-state kinetic parameters for incorporation of a nucleotide opposite both cross-linked T and G and compared them with the same for the control (Table 2). Compared to unmodified T, where dAMP was incorporated at least 2 orders of magnitude more efficiently, incorporation of dAMP opposite the cross-linked T was only 2−3-fold more efficient than a wrong dNMP incorporation. The preference for incorporation of dCMP opposite the cross-linked G was also reduced, although the magnitude was less pronounced. Opposite both the cross-linked G and T, therefore, incorporation of the correct nucleotide was preferred, though discrimination against the wrong incorporation was less efficient than a control. Next, we evaluated extension of a correct (C opposite cross-linked G) and incorrect (A opposite cross-linked G) pair in the presence of all four dNTPs. As shown in Figure 7 (left panel), for the control, the correct (G•C) pair rapidly extended to a full length 20-mer, whereas the same for the G[8,5-Me]T template progressed much more slowly. We noted that some of the full-length product further extended to a 21-mer in the case of G[8,5-Me]T but no further extension of the 20-mer occurred for the control. For a mismatched (G•A) pair, extension of the control was inefficient (Figure 7, right panel), whereas for G[8,5-Me]T, it was only slightly more inefficient than that of the correct pair. It suggests that following either correct or wrong nucleotide incorporation opposite the cross-linked G, further extension might occur at a comparable rate. We also evaluated the efficiency of extension of a C•A mismatch of the Cyt immediately 5′ to G[8,5-Me]T, which was a hot spot for C → T mutations in COS and 293T cells. Full-length extension of the primer on control and cross-linked template occurred, but both occurred very slowly. The steady-state kinetic data for incorporation of a nucleotide opposite the Gua immediately 3′ to G[8,5-Me]T (Table 3) indicated that dCMP was incorporated at least 2 orders of magnitude more efficiently than either dGMP or dAMP, whereas the same for the control was at least 3 orders of magnitude more efficient (Table 3).

In summary, hpol η exhibited the same order of nucleotide incorporation opposite each of the G[8,5-Me]T cross-link sites and their 3′ and 5′ neighboring bases as it did opposite the control, but in each case, its ability to discriminate against the wrong nucleotide was reduced relative to a control template. While this in vitro work was in progress, an article by Wang and co-workers was published (*13*) in which in vitro replication of the G[8,5-Me]T lesion by yeast DNA polymerase η was reported. In contrast to our results with hpol η, in which incorporation of the correct nucleotide was preferred opposite both the cross-linked bases, yeast pol η was much more error-prone, and insertion of dAMP and dGMP opposite the cross-linked G was favored over that of the correct nucleotide, dCMP. To reconcile these differences in nucleotide incorporation pattern between yeast and human pol η, we have determined the fidelity of nucleotide incorporation opposite cross-linked G by yeast pol η using conditions similar to those in our experiments with hpol η. The results listed in Table 4 clearly established that the F_{inc} pattern by yeast pol η in our study was nearly identical to what Wang and co-workers have reported (*13*), even though our experimental conditions were not exactly the same as those of the published work (e.g., enzyme concentration and temperature were different). Although both yeast and human pol η accurately replicate through a T−T photodimer by inserting two A nucleotides opposite the cross-linked thymines (*29*), we conclude that the two enzymes replicate a G[8,5-Me]T cross-link very differently.

DISCUSSION

DNA−DNA intrastrand cross-links such as G[8,5-Me]T and T[5-Me,8]G are likely to cause significant distortion in DNA. Both molecular modeling and thermal melting studies suggest a significant destabilizing effect of G[8,5-Me]T on the DNA duplex (*17*). Therefore, it is not surprising that G[8,5-Me]T is recognized by the NER proteins (*16, 17*) and that it strongly blocks replication in vitro (*18*). However, the cellular effects of these lesions have not been reported. The primary objective of this study is to determine if these lesions are mutagenic in mammalian cells. We also were interested in comparing mutagenesis of the two isomeric lesions in which Gua is located either 5′ or 3′ to Thy, because a preliminary molecular modeling study suggests significant difference in the orientation of the bases in the two cross-links (data not shown). We incorporated the lesions in the DNA sequence from p53 codon 272−274, in which G[8,5-Me]T was located in the codon 273 mutational hot spot (*30*), whereas the T[5-Me,8]G cross-link was situated at the third base of codon 273 and the first base of codon 274.

The mutational spectra in both COS-7 and 293T cells exhibited a unique pattern for each cross-link. Both G[8,5-Me]T and T[5-Me,8]G induced high frequencies of semi-targeted or locally targeted mutations in addition to targeted mutations. In fact, in both 293T and COS-7 cells, G[8,5-Me]T induced a higher frequency of semitargeted mutations than targeted mutations (Figures 3 and 4). For T[5-Me,8]G

Table 2: Fidelity of Nucleotide Incorporation by hpol η on a G[8,5-Me]T Cross-Link-Containing Substrate and the Undamaged Substrate As Determined by Steady-State Kinetic Measurements

dNTP	V_{max} (μM /min)	K_m (μM)	V_{max}/K_m	F_{inc}
5'-GTGCG^TGTT TGTATC GCTTGCAGGGG-3' CAAACATAGCGAACp32				
G[8, 5-Me]T –containing substrate, 14mer primer (5'-CAAGCGATACAAAC-3')				
dATP	0.015+/-0.006	0.5+/-0.2	3.0×10^{-2}	1.0
dGTP	0.020+/-0.013	3.7+/-1.4	5.0×10^{-3}	0.2
dCTP	0.051+/-0.006	6.2+/-0.7	8.0×10^{-3}	0.3
dTTP	0.048+/-0.007	5.8+/-0.7	8.0×10^{-3}	0.3
Undamaged substrate, 14mer primer (5'-CAAGCGATACAAAC-3')				
dATP	0.012+/-0.001	0.07+/-0.03	0.2	1.0
dGTP	0.023+/-0.004	7.8+/-0.6	3.0×10^{-3}	1.4×10^{-2}
dCTP	0.024+/-0.003	4.4+/-0.7	5.0×10^{-3}	2.7×10^{-2}
dTTP	0.031+/-0.007	10.8+/- 0.3	3.0×10^{-3}	1.4×10^{-2}
5'-GTGCG^TGTT TGTATC GCTTGCAGGGG-3' ACAAACATAGCGAACp32				
G[8, 5-Me]T –containing substrate, 15mer primer (5'-CAAGCGATACAAACA-3')				
dATP	0.028+/-0.014	1.3+/-0.3	2.1×10^{-2}	4.3×10^{-2}
dGTP	0.020+/-0.022	1.0+/-1.7	2.0×10^{-2}	4.0×10^{-2}
dCTP	0.039+/-0.007	0.08+/-0.05	0.5	1.0
dTTP	0.059+/-0.014	1.2+/-0.8	5.0×10^{-2}	0.1
Undamaged substrate, 15mer primer (5'-CAAGCGATACAAACA-3')				
dATP	0.037+/-0.003	6.0+/-0.5	6.0×10^{-3}	4.0×10^{-3}
dGTP	0.041+/-0.0001	12+/-3	3.0×10^{-3}	2.1×10^{-3}
dCTP	0.049+/-0.006	0.03+/-0.01	1.6	1.0
dTTP	0.050+/-0.001	20+/-6	2.0×10^{-3}	1.6×10^{-3}

in 293T cells, targeted and semitargeted single-base substitutions occurred at approximately the same frequency, whereas in COS-7 cells, targeted mutations were a bit more frequent than semitargeted mutations (Figures 3 and 5). The semitargeted mutations were localized two bases 5′ and three bases 3′ to G[8,5-Me]T, whereas they occurred three bases 5′ and three bases 3′ to T[5-Me,8]G (Figures 4 and 5). Furthermore, in 293T cells, the highest frequency of semitargeted mutations occurred at the base immediately 5′ to the lesion, which involved a C → T substitution for G[8,5-Me]T and a G → T substitution for T[5-Me,8]G (Figures 4 and 5). In COS cells, for G[8,5-Me]T the frequency of semitargeted mutations was nearly 3 times that of the targeted base substitutions, which occurred at the 3′ Gua adjacent to the lesion and at the Thy three bases 3′, in addition to the 5′ neighboring Cyt (Figure 4). By contrast, semitargeted mutations were less frequent for T[5-Me,8]G in COS cells (Figure 5). Multiple-base substitutions at or near the lesion were detected at a frequency of 1−3%. For both lesions, base substitutions were predominant, but frameshifts also occurred at a frequency of <5%.

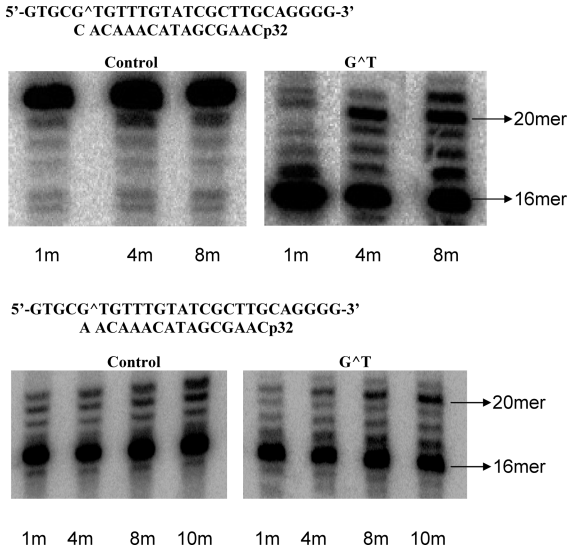

FIGURE 7: Extension of a 16-mer primer at 37 °C by hpol η (50 nM) with either a terminal 3′-C·G pair or a A·G mismatch in the presence of all four dNTPs (25 mM each).

Many bulky adducts, such as the adducts derived from benzo[*a*]pyrene diol epoxide (*31, 32*), *N*-acetyl-2-aminofluorene (*33, 34*), 2-hydroxyestrogen (*35*), and 1-nitropyrene (*36*), have been shown to cause mainly targeted G → T transversions in COS cells. Additional targeted mutations at lower frequencies occur in some of these cases. Other types of lesions, such as ethenoadenine (*26*), which contains an aromatic ring in the Watson−Crick base pairing region of adenine, and abasic site (*22, 37*), a noninstructional lesion, also induce targeted mutations. Indeed, for many replication blocking lesions, targeted mutations are predominant, and semitargeted or untargeted mutations, if any, have been detected at a very low frequency. Even so, there are a few reports about adduct-induced semitargeted mutations in specific DNA sequences. The C8-Gua adduct of *N*-acetyl-2-aminofluorene at G_1 or G_2 (but not G_3) of the sequence

Table 3: Fidelity of Nucleotide Incorporation by hpol η at the 3′-G on a G[8,5-Me]T Cross-Link-Containing Substrate and the Undamaged Substrate As Determined by Steady-State Kinetic Measurements

dNTP	V_{max} (μM /min)	K_m (μM)	V_{max}/K_m	F_{inc}
5'-GTGCG^TGTT TGTATC GCTTGCAGGGG-3' AAACATAGCGAACGTCp32				
G[8, 5-Me]T –containing substrate, 16mer primer (5'-CTGCAAGCGATACAAA -3')				
dATP	0.067+/- 0.00014	0.76+/- 0.032	0.08	1.0×10^{-2}
dGTP	0.076+/- 0.00036	0.27+/- 0.032	0.28	3.1×10^{-2}
dCTP	0.117+/- 0.00022	0.01+/- 0.001	11.7	1.0
dTTP	0.087+/- 0.00001	4.22+/- 0.003	0.02	2.3×10^{-3}
Undamaged substrate, 16mer primer (5'- CTGCAAGCGATACAAA -3')				
dATP	0.051+/- 0.00025	0.34+/- 0.03	0.15	4.8×10^{-3}
dGTP	0.121+/- 0.0013	3.11+/- 0.11	0.04	1.3×10^{-3}
dCTP	0.124+/- 0.00035	$0.004+/- 7.1 \times 10^{-5}$	31.00	1.0
dTTP	0.094+/- 0.00011	5.16+/-0.09	0.02	6.4×10^{-4}

Table 4: Fidelity of Nucleotide Incorporation by Yeast pol η on a G[8,5-Me]T Cross-Link-Containing Substrate As Determined by Steady-State Kinetic Measurements

dNTP	V_{max} (μM /min)	K_m (μM)	V_{max}/K_m	F_{inc}
5'-GTGCG^TGTT TGTATC GCTTGCAGGGG-3' ACAAACATAGCGAACp32				
G[8, 5-Me]T –containing substrate, 15mer primer (5'-CAAGCGATACAAACA-3')				
dATP	0.042+/-0.002	145+/-3	8.2×10^{-3}	1.0
dGTP	0.046+/- 0.001	61.4+/-0.1	4.0×10^{-3}	0.5
dCTP	0.044+/-0.0001	7.4+/-0.7	2.9×10^{-4}	3.5×10^{-2}
dTTP	0.046+/- 0.002	5.6+/-1.2	7.4×10^{-4}	9.0×10^{-2}

context 5′-CCCG$_1$G$_2$G$_3$-3′ induces a one-base deletion in the run of three cytosines (*38*). (+)-*trans-anti*-Benzo[*a*]pyrene-N^2-guanine in the sequence 5′-CG$_1$G$_2$C-3′ causes semitargeted G$_2$ → A substitutions when the adduct is located at G$_1$ (*39*). In contrast to O^6-methylguanine, which induces only targeted mutations, O^6-ethylguanine and O^6-benzylguanine induce both targeted and semitargeted base substitutions (*40*), but specifically with respect to mutagenesis data of the radiation-induced intrastrand cross-links described here, one particular study is of interest, in which mutagenicity of the thymine−thymine 6−4 photoproduct was investigated (*41*). The thymine−thymine 6−4 lesion induces a high frequency (60%) of mutations in COS-7 cells, and 80% of the mutations involve G → T transversions at the 5′ Gua adjacent to the photoproduct (*41*). It is interesting that this semitargeted mutation does not occur in appreciable frequency in *E. coli* (*41*). The fact that a 6−4 photoproduct and T[5-Me,8]G are intrastrand cross-links and both cause G → T mutations at the 5′ adjacent Gua suggests that these two lesions might induce mutagenesis by a similar mechanism.

As in the case of the thymine−thymine 6−4 photoproduct (*41*), the base substitutions at or near the cross-links are consistent with the A-rule (*27, 28*), even though a large number of mutations were detected in the local region. One explanation for the complex mutation data in COS-7 and 293T cells is TLS by a highly error-prone DNA polymerase that made errors in nucleotide incorporation not only opposite the lesion but also opposite natural DNA bases near the cross-link site. pol η, a member of the Y-family of polymerases, is a candidate, because it not only can bypass many types of DNA damage but also is a low-fidelity enzyme (*42*). Both human and yeast pol η the bypass T−T photodimer efficiently and accurately (*29, 43–45*), even though yeast pol η cannot bypass N^2-Gua-N^2-Gua intrastrand cross-links formed by 1,3-butadiene metabolites (*46*), but the yeast enzyme bypasses G[8,5-Me]T and G[8,5]C cross-links (*13, 15*). We have therefore carried out an in vitro bypass study of G[8,5-Me]T in the same sequence with hpol η. The in vitro experiments showed that, unlike many other DNA polymerases that are blocked by G[8,5-Me]T, hpol η can bypass the cross-link. Though the bypass was much slower than a control, this Y-family polymerase incorporated the correct dNMP opposite each cross-linked base. The incorporation of correct nucleotide, dAMP, opposite cross-linked T was 3−5-fold more efficient than that of a wrong nucleotide, whereas dCMP incorporation opposite the cross-linked G was 10-fold more efficient than dTMP incorporation. Further extension following misincorporation of A opposite the cross-linked G was also evaluated in comparison to C opposite it, which showed that C opposite the cross-linked G was preferred but the discrimination to extend the wrong base was far less stringent than the control. Fidelity of nucleotide incorporation opposite the 3′ base to G[8,5-Me]T was also evaluated to determine if the semitargeted base substitutions

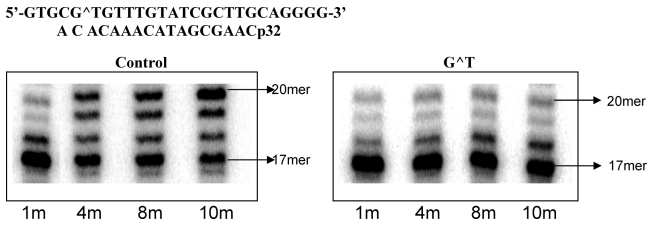

FIGURE 8: Extension of a 17-mer primer at 37 °C by hpol η (50 nM) with a terminal 3′-A•C mismatch in the presence of all four dNTPs (25 mM each).

can be rationalized. We found that discrimination to incorporate the correct nucleotide was 10-fold lower at this site relative to a control. However, incorporation of a nucleotide by hpol η does not appear to be consistent with the observed cellular mutations. On the contrary, a part of the wild-type progeny could have been derived from the cross-linked vector by error-free bypass by hpol η.

The observation that hpol η preferentially incorporated the correct nucleotide opposite each of the cross-linked bases is in stark contrast to the results of a recent study using yeast pol η, which is highly error-prone in nucleotide incorporation opposite the cross-linked G (*13*). We were able to reproduce this result using conditions similar to those in our in vitro experiment with hpol η, which confirmed that the yeast and human pol η behave quite differently in TLS of G[8,5-Me]T. This is not surprising because several studies have established differences between the yeast and human enzymes. For TLS of γ-hydroxypropanodeoxyguanosine by these two polymerases, yeast pol η synthesizes past the adduct relatively accurately, whereas human pol η discriminates poorly between incorporation of correct and wrong nucleotides opposite the adduct (*47*). Prakash and co-workers have examined the mechanistic basis of these two enzymes and found that they differ in several important respects (*48*). Human pol η has a 50-fold faster rate of nucleotide incorporation than yeast pol η but binds the nucleotide with an approximately 50-fold lower affinity (*48*).

In conclusion, the intrastrand cross-links G[8,5-Me]T and T[5-Me,8]G are significantly mutagenic in simian and human embryonic kidney cells. T[5-Me,8]G induced a higher frequency of targeted base substitutions than G[8,5-Me]T did, but both lesions caused a wide variety of mutations at or near the cross-link, including single- and multiple-base substitutions as well as small frameshifts. We believe that this unique signature of mutational spectra of these lesions arises from TLS by a highly error-prone DNA polymerase. In vitro bypass by hpol η indicated that the fidelity of this low-fidelity polymerase at or near the cross-links was further reduced, but the types of mutations detected in cells did not correspond well with the results of our bypass study. We believe that either another Y-family DNA polymerase or an accessory protein plays a critical role in the mutagenicity of these cross-links. However, we cannot rule out the possibility that hpol η may be responsible for correct bypass of the cross-links.

SUPPORTING INFORMATION AVAILABLE

Mutation data in 293T and COS-7 cells, representative autoradiograms, and Hanes−Woolf plots for steady-state kinetic measurements. This material is available free of charge via the Internet at http://pubs.acs.org.

REFERENCES

1. Finkel, T., and Holbrook, N. J. (2000) Oxidants, oxidative stress and the biology of ageing. *Nature 408*, 239–247.
2. Evans, M. D., Dizdaroglu, M., and Cooke, M. S. (2004) Oxidative DNA damage and disease: Induction, repair and significance. *Mutat. Res. 567*, 1–61.
3. Wang, Y. (2008) Bulky DNA lesions induced by reactive oxygen species. *Chem. Res. Toxicol. 21*, 276–281.
4. Box, H. C., Budzinski, E. E., Dawidzik, J. B., Gobey, J. S., and Freund, H. G. (1997) Free radical-induced tandem base damage in DNA oligomers. *Free Radical Biol. Med. 23*, 1021–1030.
5. Box, H. C., Budzinski, E. E., Dawidzik, J. D., Wallace, J. C., Evans, M. S., and Gobey, J. S. (1996) Radiation-induced formation of a crosslink between base moieties of deoxyguanosine and thymidine in deoxygenated solutions of d(CpGpTpA). *Radiat. Res. 145*, 641–643.
6. Budzinski, E. E., Dawidzik, J. B., Rajecki, M. J., Wallace, J. C., Schroder, E. A., and Box, H. C. (1997) Isolation and characterization of the products of anoxic irradiation of d(CpGpTpA). *Int. J. Radiat. Biol. 71*, 327–336.
7. Box, H. C., Budzinski, E. E., Dawidzik, J. B., Wallace, J. C., and Iijima, H. (1998) Tandem lesions and other products in X-irradiated DNA oligomers. *Radiat. Res. 149*, 433–439.
8. Bellon, S., Ravanat, J. L., Gasparutto, D., and Cadet, J. (2002) Cross-linked Thy-purine base tandem lesions: Synthesis, characterization, and measurement in γ-irradiated isolated DNA. *Chem. Res. Toxicol. 15*, 598–606.
9. Zhang, Q., and Wang, Y. (2003) Independent generation of 5-(2′-deoxycytidinyl)methyl radical and the formation of a novel cross-link lesion between 5-methylCyt and Gua. *J. Am. Chem. Soc. 125*, 12795–12802.
10. Zhang, Q., and Wang, Y. (2004) Independent generation of the 5-hydroxy-5,6-dihydrothymidin-6-yl radical and its reactivity in dinucleoside monophosphates. *J. Am. Chem. Soc. 126*, 13287–13297.
11. Zhang, Q., and Wang, Y. (2005) The reactivity of the 5-hydroxy-5,6-dihydrothymidin-6-yl radical in oligodeoxyribonucleotides. *Chem. Res. Toxicol. 18*, 1897–1906.
12. Carter, K. N., and Greenberg, M. M. (2003) Tandem lesions are the major products resulting from a pyrimidine nucleobase radical. *J. Am. Chem. Soc. 125*, 13376–13378.
13. Jiang, Y., Hong, H., and Wang, Y. (2007) In-vivo formation and in-vitro replication of a Gua-Thy intrastrand cross-link lesion. *Biochemistry 46*, 12757–12763.
14. Hong, H., Cao, H., and and Wang, Y. (2007) Formation and genotoxicity of a Gua Cyt intrastrand cross-link lesion in vivo. *Nucleic Acids Res. 35*, 7118–7127.
15. Gu, C., and Wang, Y. (2004) LC-MS/MS identification and yeast polymerase η bypass of a novel γ-irradiation-induced intrastrand cross-link lesion G[8-5]C. *Biochemistry 43*, 6745–6750.
16. Yang, Z., Colis, L. C., Basu, A. K., and Zou, Y. (2005) Recognition and incision of γ-radiation-induced cross-linked Gua-Thy tandem lesion G[8,5-Me]T by UvrABC nuclease. *Chem. Res. Toxicol. 18*, 1339–1346.
17. Gu, C., Zhang, Q., Yang, Z., Wang, Y., Zou, Y., and Wang, Y. (2006) Recognition and incision of oxidative intrastrand cross-link lesions by UvrABC nuclease. *Biochemistry 45*, 10739–10746.
18. Bellon, S., Gasparutto, D., Saint-Pierre, C., and Cadet, J. (2006) Gua-Thy intrastrand cross-linked lesion containing oligonucleotides: From chemical synthesis to *in vitro* enzymatic replication. *Org. Biomol. Chem. 4*, 3831–3837.
19. McNulty, J. M., Jerkovic, B., Bolton, P. H., and Basu, A. K. (1998) Replication inhibition and miscoding properties of DNA templates containing a site-specific *cis*-Thy glycol or urea residue. *Chem. Res. Toxicol. 11*, 666–673.
20. Moriya, M. (1993) Single-stranded shuttle phagemid for mutagenesis studies in mammalian cells: 8-Oxoguanine in DNA induces targeted G•C → T•A transversions in simian kidney cells. *Proc. Natl. Acad. Sci. U.S.A. 90*, 1122–1126.
21. Hirt, B. (1967) Selective extraction of polyoma DNA from infected mouse cell cultures. *J. Mol. Biol. 26*, 365–369.
22. Kalam, M. A., and Basu, A. K. (2005) Mutagenesis of 8-oxoguanine adjacent to an abasic site in simian kidney cells: Tandem mutations and enhancement of G→T transversions. *Chem. Res. Toxicol. 18*, 1187–1192.
23. Boosalis, M. S., Petruska, J., and Goodman, M. F. (1987) DNA polymerase insertion fidelity: Gel assay for site-specific kinetics. *J. Biol. Chem. 262*, 14689–14696.

24. Randall, S. K., Eritja, R., Kaplan, B. E., Petruska, J., and Goodman, M. F. (1987) Nucleotide insertion kinetics opposite abasic lesions in DNA. *J. Biol. Chem. 262*, 6864–6870.
25. Mendelman, L. V., Petruska, J., and Goodman, M. F. (1990) Base mispair extension kinetics. *J. Biol. Chem. 265*, 2338–2346.
26. Pandya, G. A., and Moriya, M. (1996) 1,N^6-Ethenodeoxyadenosine, a DNA adduct highly mutagenic in mammalian cells. *Biochemistry 35*, 11487–11492.
27. Strauss, B. S. (1991) The 'A rule' of mutagen specificity: A consequence of DNA polymerase bypass of non-instructional lesions? *BioEssays 13*, 79–84.
28. Randall, S. K., Eritja, R., Kaplan, B. E., Petruska, J., and Goodman, M. F. (1987) Nucleotide insertion kinetics opposite abasic lesions in DNA. *J. Biol. Chem. 262*, 6864–6870.
29. Johnson, R. E., Washington, M. T., Prakash, S., and Prakash, L. (1999) Bridging the gap: A family of novel DNA polymerases that replicate faulty DNA. *Proc. Natl. Acad. Sci. U.S.A. 96*, 12224–12226.
30. Hollstein, M., Shomer, B., Greenblatt, M., Soussi, T., Hovig, E., Montesano, R., and Harris, C. C. (1996) Somatic point mutations in the p53 gene of human tumors and cell lines: Updated compilation. *Nucleic Acids Res. 24*, 141–146.
31. Moriya, M., Spiegel, S., Fernandes, A., Amin, S., Liu, T., Geacintov, N., and Grollman, A. P. (1996) Fidelity of translesional synthesis past benzo[*a*]pyrene diol epoxide-2′-deoxyguanosine DNA adducts: Marked effects of host cell, sequence context, and chirality. *Biochemistry 35*, 16646–16651.
32. Dong, H., Bonala, R. R., Suzuki, N., Johnson, F., Grollman, A. P., and Shibutani, S. (2004) Mutagenic potential of benzo[*a*]pyrene-derived DNA adducts positioned in codon 273 of the human *p53* gene. *Biochemistry 43*, 15922–15928.
33. Shibutani, S., Suzuki, N., and Grollman, A. P. (1998) Mutagenic specificity of (acetylamino)fluorene-derived DNA adducts in mammalian cells. *Biochemistry 37*, 12034–12041.
34. Shibutani, S., Suzuki, N., Tan, X., Johnson, F., and Grollman, A. P. (2001) Influence of flanking sequence context on the mutagenicity of acetylaminofluorene-derived DNA adducts in mammalian cells. *Biochemistry 40*, 3717–3722.
35. Terashima, I., Suzuki, N., and Shibutani, S. (2001) Mutagenic properties of estrogen quinone-derived DNA adducts in simian kidney cells. *Biochemistry 40*, 166–172.
36. Watt, D. L., Utzat, C. D., Hilario, P., and Basu, A. K. (2007) Mutagenicity of the 1-nitropyrene-DNA adduct *N*-(deoxyguanosin-8-yl)-1-aminopyrene in mammalian cells. *Chem. Res. Toxicol. 20*, 1658–1664.
37. Gentil, A., Cabral-Neto, J. B., Mariage-Samson, R., Margot, A., Imbach, J. L., Rayner, B., and Sarasin, A. (1992) Mutagenicity of a unique apurinic/apyrimidinic site in mammalian cells. *J. Mol. Biol. 227*, 981–984.
38. Lambert, I. B., Napolitano, R. L., and Fuchs, R. P. P. (1992) Carcinogen-induced frameshift mutagenesis in repetitive sequence. *Proc. Natl. Acad. Sci. U.S.A. 89*, 1310–1314.
39. Jelinsky, S. A., Mao, B., Geacintov, N. E., and Loechler, E. L. (1995) The major N^2-Gua adduct of the (+)-*anti*-benzo[a]pyrene diol epoxide is capable of inducing G → A and G → C in addition to G → T, mutations. *Biochemistry 34*, 13545–13553.
40. Bishop, R. E., Pauly, G. T., and Moschel, R. C. (1996) O^6-Ethylguanine and O^6-benzylguanine incorporated site-specifically in codon 12 of the rat H-*ras* gene induce semi-targeted as well as targeted mutations in Rat4 cells. *Carcinogenesis 17*, 849–856.
41. Gentil, A., Le Page, F., Margot, A., Lawrence, C. W., Borden, A., and Sarasin, A. (1996) Mutagenicity of a unique thymine-thymine dimer or thymine-thymine pyrimidine pyrimidone (6−4) photoproduct in mammalian cells. *Nucleic Acids Res. 24*, 1837–1840.
42. Prakash, S., and Prakash, L. (2002) Translesion DNA synthesis in eukaryotes: A one- or two-polymerase affair. *Genes Dev. 16*, 1872–1883.
43. Washington, M. T., Johnson, R. E., Prakash, L., and Prakash, S. (2000) Accuracy of thymine-thymine dimer bypass by *Saccharomyces cerevisiae* DNA polymerase η. *Proc. Natl. Acad. Sci. U.S.A. 97*, 3094–3099.
44. Washington, M. T., Prakash, L., and Prakash, S. (2003) Mechanism of nucleotide incorporation opposite a thymine-thymine dimer by yeast DNA polymerase η. *Proc. Natl. Acad. Sci. U.S.A. 100*, 12093–12098.
45. Johnson, R. E., Prakash, L., and Prakash, S. (2005) Distinct mechanisms of cis-syn thymine dimer bypass by Dpo4 and DNA polymerase η. *Proc. Natl. Acad. Sci. U.S.A. 102*, 12359–12364.
46. Minko, I. G., Washington, M. T., Kanuri, M., Prakash, L., Prakash, S., and Lloyd, R. S. (2003) Translesion synthesis past acrolein-derived DNA adduct, γ-hydroxypropanodeoxyguanosine, by yeast and human DNA polymerase η. *J. Biol. Chem. 278*, 784–790.
47. Minko, I. G., Washington, M. T., Prakash, L., Prakash, S., and Lloyd, R. S. (2001) Translesion DNA synthesis by yeast DNA polymerase η on templates containing N^2-Gua adducts of 1,3-butadiene metabolites. *J. Biol. Chem. 276*, 2517–2522.
48. Washington, M. T., Johnson, R. E., Prakash, L., and Prakash, S. (2003) The mechanism of nucleotide incorporation by human DNA polymerase η differs from that of the yeast enzyme. *Mol. Cell. Biol. 23*, 8316–8322.

BI800529F